




# Improved Voltammetric Determination of Kynurenine at the Nafion Covered Glassy Carbon Electrode – Application in Samples Delivered from Human Cancer Cells

International Journal of Tryptophan Research  
Volume 14: 1–14  
© The Author(s) 2021  
Article reuse guidelines:  
sagepub.com/journals-permissions  
DOI: 10.1177/11786469211023468  


Ilona Sadok<sup>1</sup> , Katarzyna Tyszczyk-Rotko<sup>2</sup>, Robert Mroczka<sup>3</sup>,  
Jędrzej Kozak<sup>2</sup> and Magdalena Staniszewska<sup>1</sup> 

<sup>1</sup>Laboratory of Separation and Spectroscopic Method Applications, Centre for Interdisciplinary Research, Faculty of Science and Health, The John Paul II Catholic University of Lublin, Lublin, Poland. <sup>2</sup>Institute of Chemical Sciences, Faculty of Chemistry, Maria Curie-Skłodowska University in Lublin, Lublin, Poland. <sup>3</sup>Laboratory of X-ray Optics, Centre for Interdisciplinary Research, Faculty of Science and Health, The John Paul II Catholic University of Lublin, Lublin, Poland.

**ABSTRACT:** Nowadays, development of analytical methods responding to a need for rapid and accurate determination of human metabolites is highly desirable. Herein, an electrochemical method employing a Nafion-coated glassy carbon electrode (Nafion/GCE) has been developed for reliable determination of kynurenine (a key tryptophan metabolite) using a differential pulse adsorptive stripping voltammetry. To our knowledge, this is the first analytical method to allow for kynurenine determination at the Nafion-coated electrode. The methodology involves kynurenine pre-concentration in 0.1 M H<sub>2</sub>SO<sub>4</sub> in the Nafion film at the potential of +0.5 V and subsequent stripping from the electrode by differential pulse voltammetry. Under optimal conditions, the sensor can detect 5 nM kynurenine (for the accumulation time of 60 seconds), but the limit of detection can be easily lowered to 0.6 nM by prolonging the accumulation time to 600 seconds. The sensor shows sensitivity of 36.25 μA μM<sup>-1</sup> cm<sup>-2</sup> and 185.50 μA μM<sup>-1</sup> cm<sup>-2</sup> for the accumulation time of 60 and 600 seconds, respectively. The great advantage of the proposed method is easy sensor preparation, employing drop coating method, high sensitivity, short total analysis time, and no need for sample preparation. The method was validated for linearity, precision, accuracy (using a high-performance liquid chromatography), selectivity (towards tryptophan metabolites and different amino acids), and recovery. The comprehensive microscopic and electrochemical characterization of the Nafion/GCE was also conducted with different methods including atomic force microscopy (AFM), optical profilometry, time-of-flight secondary ion mass spectrometry (TOF-SIMS), electrochemical impedance spectroscopy (EIS), and cyclic voltammetry (CV). The method has been applied with satisfactory results for determination of kynurenine concentration in a culture medium collected from the human ovarian carcinoma cells SK-OV-3 and to measure IDO enzyme activity in the cancer cell extracts.

**KEYWORDS:** Kynurenine, tryptophan metabolites analysis, kynurenine pathway, Nafion modified electrodes, adsorptive stripping voltammetry, cancer cells

**RECEIVED:** December 15, 2020. **ACCEPTED:** May 3, 2021.

**TYPE:** Original Research

**FUNDING:** The author(s) disclosed receipt of the following financial support for the research, authorship, and/or publication of this article: This work was supported by grant from the National Science Centre, Poland for Ilona Sadok (Grant No. 2018/02/X/ST4/00187) and for Magdalena Staniszewska (OPUS13, Grant No. 2017/25/B/NZ4/01198) as well as funding from the European Union from European Regional Development Fund under the Operational Programme Development of Eastern Poland 2007-2013 (agreement POPW.01.03.00-06-003/09-00).

**DECLARATION OF CONFLICTING INTERESTS:** The author(s) declared no potential conflicts of interest with respect to the research, authorship, and/or publication of this article.

**CORRESPONDING AUTHOR:** Magdalena Staniszewska, Laboratory of Separation and Spectroscopic Method Applications, Centre for Interdisciplinary Research, Faculty of Science and Health, The John Paul II Catholic University of Lublin, Konstantynów 1J, Lublin 20-708, Poland. Email: magdalena.staniszewska@kul.pl

## Introduction

Kynurenine (Kyn) is the first stable metabolite of tryptophan (Trp) degradation via the kynurenine pathway (KP). Kyn is produced in a liver by tryptophan 2,3-dioxygenase enzyme (TDO) and extrahepatically by indoleamine 2,3-dioxygenase (IDO) expressed by several cell types, including cancer and immune cells.<sup>1</sup> Under physiological conditions, TDO is responsible for >95% of the overall Trp degradation. IDO contributes only at 5%–15% to this process,<sup>2</sup> however the importance of the extrahepatic pathway significantly increases under conditions of immune activation.

Kyn is a precursor for other Trp downstream metabolites, some with cytotoxic properties (like 3-hydroxykynurenine, quinolinic acid).<sup>3,4</sup> Furthermore, this molecule itself can suppress allogeneic T-cell proliferation.<sup>5</sup> Kyn is also an endogenous ligand of the human aryl hydrocarbon receptor (AHR)—the crucial factor of the immune responses regulation and cancer

progression.<sup>6</sup> Increased Kyn concentration in biological fluids has been associated with many diseases, including HIV,<sup>7</sup> lung cancer,<sup>8</sup> chronic obstructive pulmonary disease,<sup>9</sup> attention deficit hyperactivity disorder (ADHD),<sup>10</sup> and many others.

Because of the undisputed implication of KP metabolites in mechanism of many diseases, the development of accurate and rapid analytical tools for their determination in a variety of biological samples is highly desirable. Monitoring of Kyn—as the first stable KP metabolite—is one of the major factors in research focused on the relationship between KP activation and disease progression. The predominant method used for Kyn quantification in biological samples is liquid chromatography employing various detectors (including UV absorbance, fluorescence, electrochemical, and mass spectrometry).<sup>11</sup> There are several drawbacks of chromatographic methods such as the time-consuming sample preparation, expensive and sophisticated equipment, and large organic solvent usage. Meanwhile,



some developments in the design of sensors for Kyn quantification in biological samples have been reported. The molecularly imprinted two-dimensional photonic crystal hydrogel sensor working with an optic spectrometer and the fluorescent sensor based on the coumarin aldehyde scaffold for the detection of Kyn have been developed.<sup>12,13</sup> Electrochemical sensors show appreciable advantages such as rapidness, simple operation, impressive sensitivity, high selectivity, good reproducibility, easy miniaturization.<sup>14-17</sup> Recently, we have also proposed the boron-doped diamond electrode modified *in situ* with bismuth film (BiF/BDDE) in combination with the differential pulse voltammetry for simultaneous Trp and Kyn determination in the post-culture medium from cancer cells.<sup>18</sup> Some main advantages of this methodology are rapid detection (less than 60 seconds) and direct sample analysis without sample preparation. The sensor allows for Trp and Kyn detection at concentrations of 30 nM.

The goal of this study was to improve the sensitivity of the voltammetric Kyn determinations. Its quantification is challenging due to significantly lower concentration in biological samples compared to Trp. We combined the ability of preconcentration of positively charged molecules in a Nafion layer with a high sensitivity of adsorptive stripping voltammetry (AdSV) to determine lower concentrations of Kyn compared to the previous methodology using the BiF/BDDE electrode.<sup>18</sup> In AdSV, the target analyte is adsorbed onto the working electrode surface by a non-electrolytic process prior to the voltammetric measurement (stripping). Thanks to the preconcentration step, AdSV allows for working with very diluted samples and decreases some possible interferences delivered from the other matrix components.<sup>19</sup> On the other hand, Nafion is a polymer acting as an exchanger membrane and facilitates pre-concentration of cations on the electrode surface. Due to its thermal stability, chemical inertness, and mechanical strength, Nafion is widely used to modify electrodes in electrochemistry. Nafion-based sensors have been applied earlier for determination of metal ions<sup>20-24</sup> and important organic compounds<sup>25-36</sup> by AdSV. However, to our knowledge, Kyn determination using Nafion-modified electrodes has not been reported. Based on our observation, that Kyn in acidic media might be adsorbed in the Nafion layer before stripping step, we have developed a sensor—the Nafion-coated glassy carbon electrode (Nafion/GCE) that is able to detect Kyn at concentration as low as 0.6 nM by the differential pulse adsorptive stripping voltammetry (DPAdSV). Performance of the sensor has been carefully studied including electrode surface morphology characteristics, selectivity, and accuracy confirmed by high pressure liquid chromatography with diode array detection (HPLC-DAD). The Nafion/GCE can find application for measuring IDO activity or Kyn quantification in the culturing medium from cancer cells, like it has been demonstrated here on SK-OV-3 human ovarian carcinoma cells.

## Material and Methods

### *Apparatus and instrumentation*

Voltammetric determinations were performed using a potentiostat/galvanostat (PGSTAT101, Metrohm, the Netherlands) operated with a 1.11 NOVA software. The measurements were carried out using a three-electrode quartz cell (volume of 10 mL) consisting of a platinum wire (counter electrode), Ag/AgCl (reference electrode), and a working electrode. Glassy carbon electrode (GCE, Mineral, Poland) and boron-doped diamond electrode (BDDE, Windsor Scientific Ltd, Berkshire, UK) both with an inner diameter of 3 mm modified with the Nafion film or without modification were used as the working electrode. GCE and BDDE were polished daily on a Buehler polishing pad using series of alumina slurries (1.0, 0.3, and 0.05  $\mu\text{m}$ ), rinsed with water, and cleaned in an ultrasonic water bath for 2 minutes with distilled water to remove adsorbed impurities. The electrochemical impedance spectroscopy (EIS) measurements were performed using an Autolab analyzer (Eco Chemie, the Netherlands) with FRA (Frequency Response Analyzer) module controlled by the FRA 4.9 software.

The system consisting of a 1200 Series high performance liquid chromatograph equipped with a diode array detector (HPLC-DAD), autosampler, quaternary pump with vacuum degasser, and column thermostat (Agilent Technologies, USA) was used for chromatographic measurements. The separation was achieved on the Zorbax Eclipse Plus C18 rapid resolution HT ( $4.6 \times 150 \text{ mm} \times 3.5 \mu\text{m}$ ) column protected by the Zorbax Eclipse Plus-C18 ( $2.1 \times 12.5 \text{ mm} \times 5 \mu\text{m}$ ) Narrow Bore Guard Column (Agilent Technologies, Folsom, USA). Instrument control, data acquisition and analysis were performed using Agilent ChemStation software v.B.04.02. Chromatographic analysis was conducted using ultra-purified water ( $>18 \text{ M}\Omega \text{ cm}$ ) produced by a Milli-Q system (Millipore, UK).

The optical profilometer (WYKO NT9800, Veeco, USA) was used to determine the microscale morphology of the surface (microroughness) in three dimensions. The objective lens magnification was set to  $40\times$  corresponding to  $0.38 \mu\text{m}$  sampling (pixel) size. The post-processing analysis was carried out using the Probe Image Processor (SPIP) v. 5.1.4 software (Image Metrology A/S, Denmark).

Nanoscale morphology was assessed by atomic force microscopy using the 5600 LS AFM instrument (Agilent Technologies). Surface scanning was conducted in the non-contact mode using the tip with a radius  $<7 \text{ nm}$  and the resonance frequency of 280 kHz. AFM micrographs were recorded at a scan area size of  $2 \times 2 \mu\text{m}^2$  with a resolution of  $256 \times 256$  that corresponded to  $39 \text{ nm/pixel}$ . The vertical noise in the AFM instrument was  $\sim 0.05 \text{ nm}$ . The images were analysed in the aspect of surface height statistics, that is, the root-mean-square (Sq) commonly defined as surface roughness parameter using the Probe Image Processor (SPIP) v. 5.1.4 software (Image Metrology A/S, Denmark).

The time-of-flight secondary ion mass spectrometry (TOF-SIMS) measurements were performed on the GCE modified with Nafion layer (Nafion/GCE). The electrodes after Kyn accumulation were mounted on a home-made holder and were transferred to the TOF-SIMS instrument within 1 hour after preparation. TOF-SIMS spectra were acquired with the TOF-SIMS.5 instrument (ION-TOF GmbH, Germany) and the primary ion source of Bi<sup>+</sup> set up at 25 keV, corresponding to 1.0 pA primary beam current in spectrometry mode. The scanning area of the secondary ions was 200 μm × 200 μm with 256 × 256 pixels (1 shot/pixel). All the measurements were performed under the static mode (dose < 1 × 10<sup>12</sup> ions/cm<sup>2</sup>) in a positive-ion-mode. To neutralize the charge left on the surface, an electron flood gun (20 eV) and surface potential (-480 eV) were applied. For all samples, three different places spread out from each other by approximately 0.4 mm distance were analysed. No statistical difference was found among measurements. The post-processing data analysis was conducted using the SurfaceLab 6.7 software (ION-TOF) and Origin 2019 (OriginLab) for data recorded in Spectrometry Mode. Spectra calibration was applied using the positions of CH<sub>3</sub><sup>+</sup>, C<sub>2</sub>H<sub>3</sub><sup>+</sup>, C<sub>2</sub>H<sub>5</sub><sup>+</sup> fragments.

Human cancer cells were cultured in the HERAcell 150i Cu incubator (Thermo Fisher Scientific). Protein concentration was estimated using the multi-mode microplate reader Synergy 2 (Bio Tek Instruments Inc, Winooski, USA) operated with the Gen5 1.09 software.

Crystalline chemicals were weighed using the XP6 microbalance from Mettler Toledo (Switzerland). The pH measurements were made on the CI-316 pH meter (Elmetron) and SevenMulti™ dual meter pH/conductivity equipped with InLab® Expert Pro (Mettler Toledo, Switzerland). Samples were centrifuged using the 5415R Centrifuge (Eppendorf, Germany), and concentrated using the Genevac EZ-2 Elite Personal Evaporator (Genevac Ltd, UK).

### Reagents

Crystalline 3-hydroxy-D,L-kynurenine (3HKyn), 3-hydroxyanthranilic acid (3HAA, 97%), 5-hydroxyindoleacetic acid (5HIAA), 5-hydroxytryptamine hydrochloride (5-HT), 2-picolinic acid (PIC, 99%), L-alanine (Ala, ≥98%), anthranilic acid (AA, ≥99.5%), L-ascorbic acid (Vit C, ≥99%), L-aspartic acid (Asn, ≥98%), L-asparagine (Asp, ≥98%), L-arginine (Arg, ≥98%), citric acid (CA), dopamine hydrochloride (DOP), glucose (Glu), L-glutamine (Glu, ≥99%), glycine (Gly, ≥98.5%), indoxyl acetate (IA, ≥95%), indoxyl sulfate potassium salt (IS), kynurenic acid (Kyna, ≥98%), L-cysteine (Cys, ≥98%), L-histidine (His, ≥99%), L-kynurenine (Kyn, ≥98%), L-leucine (Leu, ≥98%), L-lysine (Lys, ≥98%), L-methionine (Met, ≥98%), L-serine (Ser, ≥99%), L-threonine (Thr, ≥98%), L-tryptophan (Trp, ≥98%), L-tyrosine (Tyr, ≥98%), L-phenylalanine (Phe, ≥98%), L-proline (Pro, ≥99%), melatonin (ME, ≥98%), nicotinamide (NAm, ≥99.5%), nicotinic

acid (NA, ≥99.5%), oxalic acid (OA), tartaric acid (TA), L-valine (Val, ≥98%), uric acid (UA, ≥99%), quinolinic acid (QA, 99%), xanthurenic acid (XA, 96%), 3-nitro-L-tyrosine (3NT), solution of D,L-lactic acid (85%-90%, w/w) and Nafion (5%, w/v) were obtained from Sigma-Aldrich (USA). Standard 3HKyn stock solutions were prepared in ultrapure water acidified to pH 2.5 with HCl (37%, Merck, Poland). UA, DOP, Tyr were dissolved in ultrapure water with NaOH (Sigma-Aldrich, USA); 3HAA, AA, IA, ME, Kyn, Kyna, Trp, XA in dimethyl sulfoxide (DMSO, Uvasol®, Merck, Germany), and 3NT in 0.1% (v/v) formic acid (LC-MS grade, Sigma-Aldrich, USA) in water. The rest of reagents were dissolved in ultrapure water. Standard working solutions at intermediate concentrations were prepared by dilution in ultrapure water.

The reagents for voltammetric studies, H<sub>2</sub>SO<sub>4</sub>, HNO<sub>3</sub>, HCl were purchased from Merck (Germany), CH<sub>3</sub>COOH and NaOH from Sigma-Aldrich (USA). The reagents for chromatographic purposes, that is, trichloroacetic acid (TCA) was purchased from Sigma-Aldrich (USA), whereas methanol (HPLC grade), CH<sub>3</sub>COONH<sub>4</sub>, and CH<sub>3</sub>COOH were from Merck (Germany).

SK-OV-3 human ovarian carcinoma cell line from American Type Culture Collection (ATCC) was cultured in medium supplemented with fetal bovine serum (FBS), L-glutamine, and penicillin/streptomycin purchased from PAN Biotech (Aidenbach, Germany). Dulbecco's Modified Eagle's Medium (DMEM) containing 4.5 g/L of D-glucose was from the Institute of Immunology and Experimental Therapy PAS (Wroclaw, Poland), and trypsin solution was from Sigma-Aldrich (St Louis, MO, USA). The sample for measuring of IDO activity was prepared with protease inhibitor cocktail, sodium L-ascorbate, bovine liver catalase, methylene blue, Na<sub>2</sub>HPO<sub>4</sub>, and KCl purchased from Sigma-Aldrich (St Louis, MO, USA), whereas NaCl, KH<sub>2</sub>PO<sub>4</sub>, and NaH<sub>2</sub>PO<sub>4</sub> were from Merck (Darmstadt, Germany). Phosphate buffered saline (PBS) was prepared by dissolving 8 g of NaCl, 0.2 g of KCl, 1.44 g of Na<sub>2</sub>HPO<sub>4</sub>, 0.24 g KH<sub>2</sub>PO<sub>4</sub> in 1 L of ultrapure water (pH 7.4 adjusted with HCl). Bradford reagent and bovine serum albumin (BSA) standard were purchased from Bio-Rad (München, Germany).

### Sensor preparation and conditions of DPAdSV measurements

Freshly cleaned surface of a GCE was modified with a Nafion film formed after applying 1.0 μL drop of the Nafion solution (0.5%, w/v) and drying on air for about 2 minutes at room temperature. Then, the Nafion-coated GCE (Nafion/GCE) was immersed in 0.1 M H<sub>2</sub>SO<sub>4</sub> (the supporting electrolyte) containing variable concentrations of Kyn. Kyn was accumulated onto the Nafion/GCE at the potential of +0.5 V for up to 600 seconds. During this step, the solution was stirred using a magnetic stirring bar. After 5 seconds equilibration, the differential pulse voltammograms (DPVs) were recorded between +0.7 and +1.3 V (step

potential: 0.01 V; modulation amplitude: 0.1 V; modulation time: 0.1 second; interval time: 0.3 second).

#### *In vitro culture of cancer cells and collection of samples*

Human ovarian cancer cells (SK-OV-3) were cultured on plates in DMEM medium supplemented with FBS, according to the protocol described earlier.<sup>37</sup> On the day of harvest, the culturing medium was collected from cells, centrifuged ( $14000 \times g$ , 5 minutes), and the supernatant was immediately frozen at  $-70^{\circ}\text{C}$  until further analysis. The cells were collected into a separate tube using a sterile cell scraper, washed with PBS, and after centrifugation ( $100 \times g$ , 5 minutes,  $4^{\circ}\text{C}$ ) the resulting cellular pellet kept on ice was immediately subjected to the protocol for IDO activity estimation.

#### *Sample preparation for IDO enzymatic activity determination*

Pellet of SK-OV-3 cells ( $0.3 \times 10^6$  per sample) was resuspended in  $100 \mu\text{L}$  of PBS containing  $1.0 \mu\text{L}$  of protease inhibitor cocktail, mixed well, and immediately subjected to 3 cycles of freezing/thawing steps in order to obtain the cytosolic protein fraction for IDO activity estimation performed as described earlier with some modifications.<sup>38</sup> After centrifugation ( $14000 \times g$ , 5 minutes,  $4^{\circ}\text{C}$ ), the obtained supernatant of cellular cytosolic fraction ( $90 \mu\text{L}$ ) was added to the reaction mixture for IDO activity assay ( $150 \mu\text{L}$ ), containing  $100 \mu\text{M}$  L-Trp and other components followed by the further steps as described earlier.<sup>39</sup> The sample (ready for IDO activity measurement) was divided into two parts—one was subjected to Kyn quantification by DPAdSV, the second for HPLC-DAD analysis (a reference method). In case of DPAdSV, Kyn content was determined by a standard addition method. Quantitative analysis by HPLC-DAD was carried out based on a matrix-matched calibration curve of Kyn peak area versus its amount [nmol] (injection volume:  $5 \mu\text{L}$ ). For DPAdSV, the sample ( $40\text{--}80 \mu\text{L}$ ) was directly injected into the supporting electrolyte ( $5 \text{mL}$ ) in a voltammetric cell. IDO activity was expressed as an amount of Kyn [nmol] produced within 1 minutes per  $1 \text{mg}$  of protein determined in the cytosolic cellular fraction.

#### *Protein measurement in the cancer cell extracts*

Protein content was estimated using Bradford's assay with BSA as a standard solution ( $1.23 \mu\text{g}/\text{mL}$ ) for the calibration curve following the procedure described earlier.<sup>37,40</sup> Each measurement was repeated three times.

#### *Preparation of culturing medium from cancer cells for DPAdSV and HPLC-DAD analysis*

Collected and frozen culturing medium from human ovarian cancer cells (SK-OV-3) was thawed at room temperature and

vortexed. DP-AdSV measurements were performed using an aliquot of medium ( $5\text{--}50 \mu\text{L}$ ) added directly to the supporting electrolyte ( $5 \text{mL}$ ) in the voltammetric cell and analysed for Kyn level generated by the cancer cells employing a standard addition method.

HPLC-DAD analysis of the culturing medium was done after pre-treatment according to the protocol described earlier with a slight modification.<sup>18</sup> The sample ( $125 \mu\text{L}$ ) was mixed with  $44.2 \mu\text{M}$  3NT (internal standard) and deproteinized with  $15 \mu\text{L}$  of 30% (w/v) TCA. After centrifugation ( $15 \text{minutes}$ ,  $14000 \times g$ ,  $4^{\circ}\text{C}$ ), the supernatant ( $125 \mu\text{L}$ ) was gently evaporated to dryness in a glass vial. The residual was dissolved in  $50 \mu\text{L}$  of an aqueous solution of  $10 \text{mM}$   $\text{CH}_3\text{COONH}_4$  (pH 4.0), transferred to a chromatographic insert vial, and immediately analysed in duplicate. Kyn concentration in experimental samples was calculated from the matrix-matched calibration curve of the ratio of Kyn/3NT peak area versus Kyn concentration [ $\mu\text{M}$ ]. The injection volume was  $10 \mu\text{L}$ .

#### *HPLC-DAD analysis*

Chromatographic separation was performed using the mobile phase composed of solvent A:  $10 \text{mM}$   $\text{CH}_3\text{COONH}_4$  in water (pH adjusted to  $4.0 \pm 0.05$  with glacial  $\text{CH}_3\text{COOH}$ ) and solvent B: 100% methanol (flow rate:  $0.5 \text{mL}/\text{minutes}$ ). The following gradient program was applied: 0-17 minutes -0% B; 17-20 minutes -0%-5% B; 20-30 minutes -5%-20% B; 30-35 minutes -20%-30% B; 35-40 minutes -30%-60% B; 40-45 minutes -60%-0% B; 45-50 minutes -0%B. Kyn was monitored with absorbance at  $360 \text{nm}$  and was eluted at retention time ( $t_r$ )  $15.5 \text{minutes}$ . To normalize Kyn concentration in the post-culture medium from cancer cells, 3NT signal was additionally measured at  $t_r = 26.5 \text{minutes}$ .

#### *Validation of DPAdSV method*

The limits of detection (LOD) and quantification (LOQ) of Kyn were calculated as a standard deviation of intercepts ( $n=3$ ) divided by the slope of the calibration function and multiplied by 3.3 or 10, respectively. The sensitivity was calculated by dividing the slope of the calibration curve by the electrochemical active surface area ( $A_s$ ) of the Nafion/GCE ( $0.08 \text{cm}^2$ ).<sup>25</sup>  $A_s$  was determined by cyclic voltammetry (CV) and the Randles-Sevcik equation (section 3.5). Intraday (repeatability) and interday precision (reproducibility) were estimated as the relative standard deviation of successive measurements of the current response for  $0.5 \mu\text{M}$  Kyn, determined on the same day or three different days, respectively. Reproducibility measurements were carried out using three individually prepared sensors. Sensor stability was expressed in percentage of mean peak current obtained for eight successive determinations of  $0.5 \mu\text{M}$  Kyn at the sensor stored for 7 days at ambient conditions in relation to the mean peak current for the freshly prepared Nafion/GCE.<sup>15</sup> Recovery was determined in culturing medium from cancer

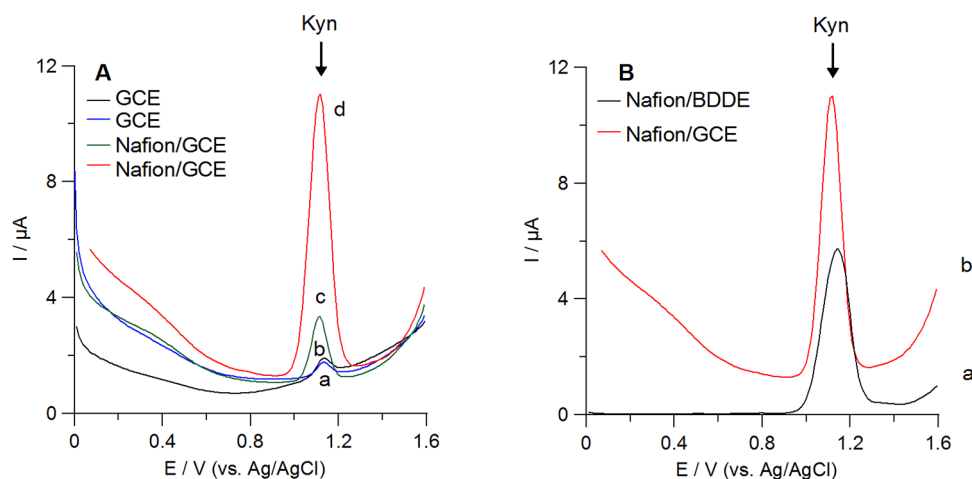


**Figure 1.** (A) Comparison of voltammetric curves obtained during determination of  $30\ \mu\text{M}$  Kyn using the bare GCE (a-b) and the Nafion film modified GCE (c-d) in  $0.1\ \text{M}\ \text{H}_2\text{SO}_4$  (scan rate  $0.02\ \text{V/s}$ ). In (b) and (d) Kyn was accumulated onto the electrode surface at potential of  $+0.75\ \text{V}$  for 60 seconds from the stirring solution. (B) DPAdSVs obtained at the Nafion covered (a) BDDE and (b) GCE after Kyn accumulation.

cells (DMEM supplemented with 10% (v/v) FBS) or reaction mixture for IDO activity measurements. The test was carried out in the supporting electrolyte (5 mL) spiked with the known amount of Kyn and aliquot of the sample. Kyn concentration was determined by the standard addition method.

#### Statistical analysis

A paired Student's *t*-test was used to evaluate differences between Kyn concentrations determined in biological samples by DPAdSV and HPLC–DAD. Data were processed using the XLSTAT 2020. The differences were considered significant at  $P < 0.05$ .

## Results and Discussion

### Preliminary electrochemical measurements

The preliminary studies were carried out in  $0.1\ \text{M}\ \text{H}_2\text{SO}_4$  serving as the supporting electrolyte with the Nafion film produced by dropping a  $1.0\ \mu\text{L}$  of 1.0% (w/v) Nafion solution onto the working electrode surface. In these conditions, Kyn is positively charged (the isoelectric point of Kyn is 6.11<sup>41</sup>). As it was demonstrated in Figure 1A, there was poor voltammetric response from Kyn on the bare GCE (line blue). After coating of the GCE surface with Nafion, there was about 5-fold increase in Kyn peak current (Figure 1A, line green). However, much more intensive increase in the Kyn peak current at the Nafion/GCE was observed after applying the additional potential ( $+0.75\ \text{V}$ , 60 seconds) during the analyte accumulation onto the electrode surface. In this case, about 22-fold enhancement of Kyn signal at the Nafion/GCE in relation to the bare GCE was observed. Comparing of the voltammograms after Kyn accumulation onto the bare GCE (Figure 1B, line black) and the Nafion/GCE (Figure 1D, line red), it is clearly seen that the Nafion membrane facilitates Kyn adsorption onto the electrode surface and ensures a significant improvement in recorded peak current. This simple modification of the working electrode surface

provides an opportunity to take advantage of adsorptive stripping voltammetry.

At this stage of studies, we have also compared Kyn signals obtained at different electrodes—GCE and BDDE. Both electrodes had the same inner diameter ( $d = 3\ \text{mm}$ ) and were modified in the same way with the Nafion film. As presented in Figure 1B, the Nafion/BDDE provides a lower background current than the Nafion/GCE. In our previous work, while developing the Kyn voltammetric sensor, we observed similar advantage in using BDDE instead of GCE.<sup>18</sup> However, using the Nafion/GCE as the working electrode resulted in better Kyn peak current and shape. Summarizing all preliminary observations, we decided to use the Nafion/GCE along with the Kyn pre-concentration step in order to develop a voltammetric methodology of Kyn determination in biological samples.

### Optimization of the Nafion/GCE preparation and conditions of Kyn determination

An effect on the Kyn peak current of the most promising supporting electrolytes  $\text{H}_2\text{SO}_4$ ,  $\text{HNO}_3$ ,  $\text{HCl}$ ,  $\text{CH}_3\text{COOH}$ , PBS (pH 3), acetic buffer (pH 4) at concentration of  $0.1\ \text{M}$  with the Nafion/GCE were tested for Kyn determination. Prior to signal recording, the analyte (Kyn) was preconcentrated onto the electrode surface at the accumulation potential of  $+0.75\ \text{V}$  for 60 seconds. Nafion film was generated by applying onto the GCE surface the  $1.0\ \mu\text{L}$  drop of 1.0% (w/v) Nafion solution. As shown in Figure 2A,  $\text{H}_2\text{SO}_4$  provided the best Kyn signal, thus this electrolyte was selected for further studies. Next, the effect of  $\text{H}_2\text{SO}_4$  concentration on Kyn peak current was also investigated in the concentration range from  $0.05$  to  $0.5\ \text{M}$  (Figure 2B). The highest Kyn signal was obtained for  $0.1\ \text{M}\ \text{H}_2\text{SO}_4$ , thus this concentration of the supporting electrolyte was selected for further measurements. Further increase of  $\text{H}_2\text{SO}_4$  concentration resulted in a significant decrease in Kyn signal.

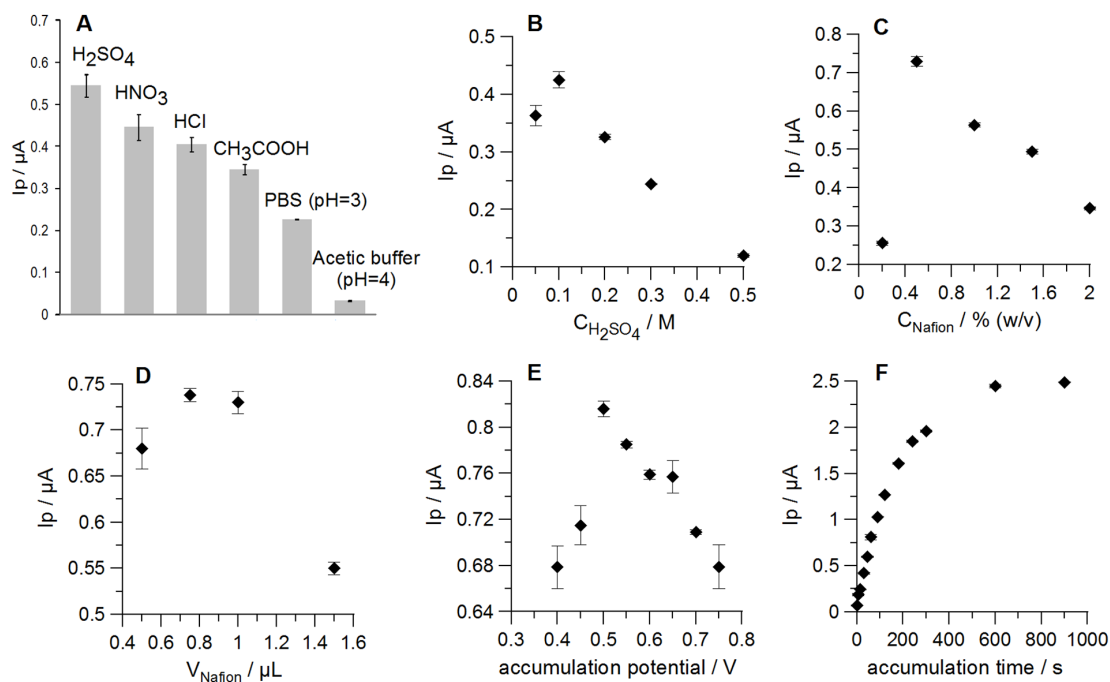


**Figure 2.** Influence of (A) the supporting electrolyte type, (B) the concentration of the supporting electrolyte, (C) the Nafion concentration in the coating solution (polymer film was generated by a 1.0  $\mu$ L drop), (D) volume of the Nafion solution (0.5%, w/v) applied onto the GCE surface, (E) Kyn accumulation potential, and (F) Kyn accumulation time on 0.5  $\mu$ M Kyn peak current. Standard deviation was calculated for  $n=3$ .

Next, the thickness of the Nafion film was adjusted by changing both the concentration and the volume of the coating solution applied onto the GCE surface. The effect of Nafion concentration in the coating solution was studied in the range from 0.2% to 2.0% (w/v) (Figure 2C). Kyn signal attained the maximum value when the Nafion membrane was developed by applying 0.5% (w/v) polymer solution onto the GCE surface and it was further used for electrode coating. Different volume of a Nafion drop used for electrode modification had different effect on Kyn peak current. The best results were obtained for the polymer layer generated by a 0.75 and 1.0  $\mu$ L of the coating solution (Figure 2D). However, a bigger drop volume (1.0  $\mu$ L) of 0.5% (w/v) Nafion solution was selected for the sensor preparation in order to ensure complete coverage of the GCE surface ( $d=3$  mm) with the polymer film.

Next, the effects of key parameters regulating Kyn accumulation in the Nafion film, such as accumulation potential and time, were studied to optimize the analyte voltammetric response. The influence of the accumulation potential on the Kyn peak current was investigated in the range from +0.4 to +0.75 V (accumulation time 60 seconds). The potential of +0.5 V provided the best efficiency of Kyn accumulation and was selected for further studies (Figure 2E). The effect of accumulation time was studied in the range from 0 to 900 seconds showing an increase in Kyn peak current with time increase up to 600 seconds.

#### Optimization of DPV parameters

At first, differential pulse and square wave voltammograms were compared to select the best registration technique for Kyn determination. Studies were carried out in the supporting

electrolyte containing 0.5  $\mu$ M Kyn (accumulation potential and time: +0.5 V, 60 seconds). DPV provided a lower background current and slightly lower peak current of Kyn compared to square wave voltammetry and was used in further studies. Next, the key parameters of DPV including step potential, modulation amplitude and time, interval time were optimized. Kyn concentration in the supporting electrolyte was 0.5  $\mu$ M. Step potential ( $\Delta E_{step}$ ) was optimized within the range of 5-35 mV, and Kyn peak currents increased with  $\Delta E_{step}$  to 30 mV. However,  $\Delta E_{step}$  higher than 10 mV resulted in a decrease of the number of points in recorded signals and their poor shapes. Thus,  $\Delta E_{step}$  equal to 10 mV was selected. Next, an effect of modulation amplitude ( $\Delta E_A$ ) was examined in the range of 10-200 mV. The maximal Kyn signal was obtained at  $\Delta E_A$  of 100 mV. Higher values of  $\Delta E_A$  yielded a weaker Kyn response, thus,  $\Delta E_A$  of 100 mV was subjected to further studies. Modulation time ( $t_{DP}$ ) was optimized in the range of 0.05-0.30 seconds and Kyn peak currents increased with  $t_{DP}$  up to 0.10 seconds and further started to decrease. That is why  $t_{DP}$  equal to 0.10 seconds was selected. Finally, an impact of interval time ( $t_{int}$ ) on Kyn response was tested in the range of 0.1-0.6 seconds. The highest Kyn signal was obtained at  $t_{int}$  of 0.3 seconds.

#### Morphology of the Nafion/GCE surface before and after Kyn accumulation

Morphology of the bare GCE was determined by optical profilometry and is presented in Figure 3A. The surface is relatively smooth, with the surface roughness of 6.33 nm determined on the area  $77.5 \times 58.1 \mu m^2$ . After Nafion layer deposition, numerous protrusions (probably unsolved polymer

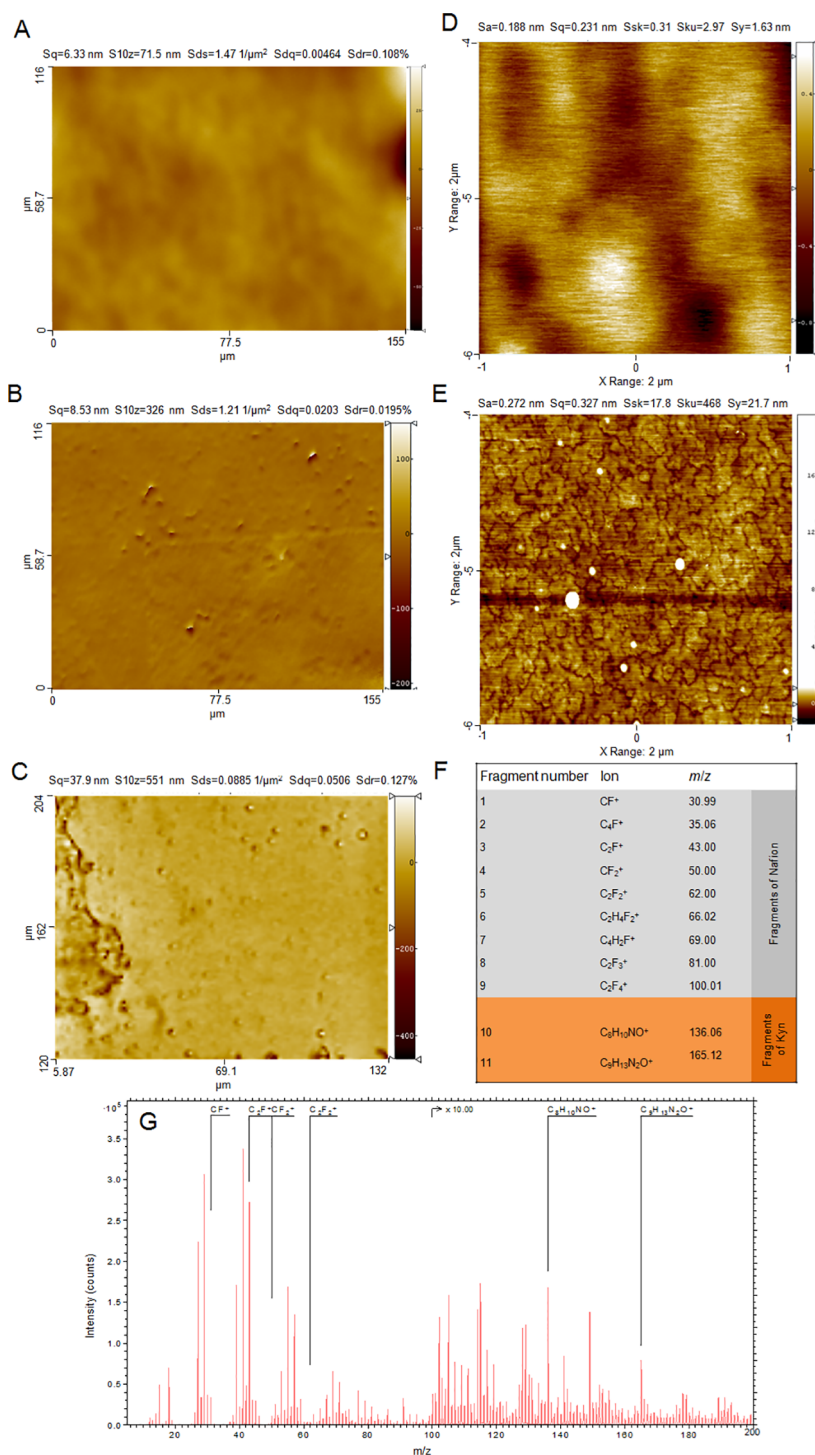


**Figure 3.** Morphology of the bare GCE (A) and GCE (B) modified with the Nafion layer (Nafion/GCE) determined by optical profilometer; scanning area:  $77.5 \times 58.1\ \mu\text{m}^2$ . (C) Optical profilometer micrographs of the Nafion/GCE surface after Kyn accumulation; scanning area:  $84 \times 126\ \mu\text{m}^2$ ; roughness parameter:  $S_q=37.9\text{ nm}$ . AFM micrographs of (D) the Nafion/GCE surface ( $S_q=0.23\text{ nm}$ ) and (E) the Nafion/GCE surface after Kyn accumulation ( $S_q=0.627\text{ nm}$ ); scanning area:  $2 \times 2\ \mu\text{m}^2$  ( $256 \times 256$  pixels). Kyn concentration in the supporting electrolyte was  $2\ \mu\text{M}$  (accumulation potential and time:  $+0.5\text{ V}$ , 60 seconds). Drop ( $1.0\ \mu\text{L}$ ) of Nafion solution (0.5%, w/v) was placed onto GCE surface. The most characteristic positive ions for Nafion and Kyn identified in TOF-SIMS spectra (F) and an example of TOF-SIMS spectra obtained for the Nafion/GCE after Kyn accumulation for 60 seconds (G) are shown.

debris) were visible, causing an increase in roughness up to about  $8.53\text{ nm}$  (Figure 3B).

The GCE surface covered by Nafion layer was also examined by AFM (Figure 3D) and showed amorphous structure in

nanoscale, while a strong tendency to waviness (deviation from flatness) in microscale was clearly seen. Kyn accumulation onto the Nafion/GCE surface resulted in the appearance of numerous crystallites (Figure 3E). The roughness parameter ( $S_q$ )

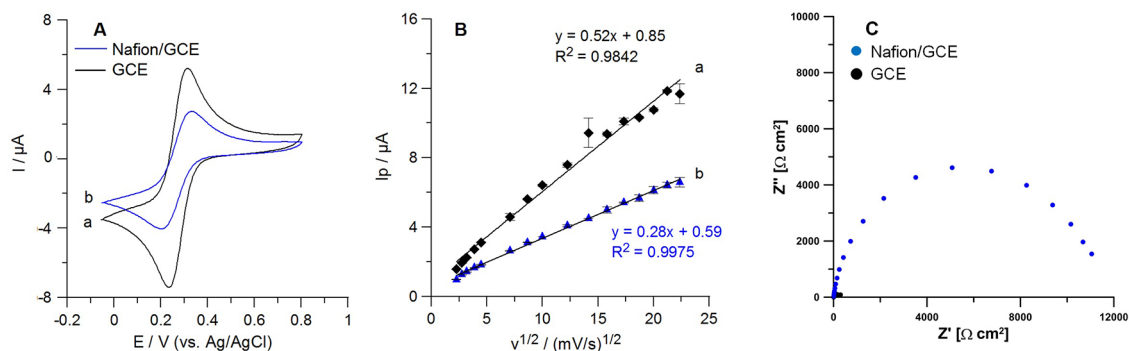


**Figure 4.** (A) Cyclic voltammograms of  $[\text{Fe}(\text{CN})_6]^{3-/4-}$  (5.0 mM containing 0.1 M KCl) recorded for the bare GCE (a) and the Nafion/GCE (b). Scan rate: 80 mV/s. (B) Dependences between  $I_p$  and  $v^{1/2}$  for the GCE (a) and the Nafion/GCE (b) in a solution of 0.1 M KCl containing 5.0 mM  $\text{K}_3[\text{Fe}(\text{CN})_6]$  (scan rate range: 5–500 mV/s). (C) Nyquist plots of the bare GCE (black) and the Nafion/GCE (blue) recorded at the potential of +0.2 V in the frequency range of 1 MHz to 0.1 Hz, in a solution of 0.1 M KCl and 5 mM  $\text{K}_3[\text{Fe}(\text{CN})_6]$ .

increased from 0.23 nm (for the Nafion/GCE) to 0.627 nm (for the Nafion/GCE after Kyn accumulation). It is worth emphasizing that the morphology of the Nafion layer in micro-scale (Figure 3B) provides information different than this from AFM microimage (Figure 3D) of a small area ( $2 \times 2 \mu\text{m}^2$ ). Moreover, AFM measurements provide information with significantly higher Lateral resolution (7.8 nm), while lateral resolution of an optical profilometer is significantly lower (120 nm). Due to this reason, AFM measurements are helpful in nanoscale morphology characterisation, whereas optical profilometer is a complementary technique for morphology on a microscale. We tried also to determine the thickness of the Nafion layer by sputtering crater with the size  $200 \times 200 \mu\text{m}^2$ . However, due to not perfectly flat GCE surface in macroscale (for areas bigger than  $1 \times 1 \text{mm}^2$ ) the results were not consistent showing relatively high standard deviation from 100 to 300 nm. After Kyn accumulation onto the Nafion/GCE surface, one can observe that surface is heterogenous (Figure 3C). On the left side, we can observe a higher accumulation of Kyn layer while on the rest of the area there are numerous small protrusions on the relatively smooth surface. Better inspection provided by AFM micrographs (Figure 3E) indicates that the Kyn layer is developed. Finally, the presence of the Nafion layer and deposition of Kyn molecules onto the Nafion/GCE surface was confirmed by TOF-SIMS measurements. Characteristic positive fragments for Nafion and Kyn species were identified in TOF-SIMS spectra (presented in Figure 3G) and are specified in Figure 3F.

#### The electrochemical characterization of the Nafion/GCE

Cyclic voltammetry (CV) in a solution of 0.1 M KCl and 5.0 mM  $\text{K}_3[\text{Fe}(\text{CN})_6]$  was employed for electrochemical characteristics of the bare GCE and the Nafion/GCE. The polymer film was obtained by applying 1.0  $\mu\text{L}$  of 0.5% (w/v) Nafion solution onto the GCE surface. As shown in Figure 4A, the CV voltammogram displayed a pair of well-defined redox peaks of  $[\text{Fe}(\text{CN})_6]^{3-/4-}$  at the bare GCE (curve a). After

modification with the polymer layer, peak-to-peak separation ( $\Delta E$ ) increased from  $71.7 \pm 0.6 \text{ mV}$  ( $n=3$ ) to  $113.3 \pm 2.9 \text{ mV}$  ( $n=3$ ), and redox peak current decreased, which ascribed to inhibition of the electrochemical reaction process by the Nafion membrane. Next, the rate of the electron transfer on the bare GCE and the Nafion/GCE was determined as the relative peak separations ( $\chi^0$ ) by dividing  $\Delta E$  by 0.059. The  $\chi^0$  values for the GCE and the Nafion/GCE were greater than the theoretical value ( $\chi^0 = 1$ ) and were equal to 1.22 and 1.92, respectively. The obtained results indicate that the Nafion film inhibits the electron transfer kinetics. The electrochemical active surfaces ( $A_s$ ) of the GCE and the Nafion/GCE were also determined based on the Randles-Sevcik equation for a reversible electrode process<sup>42</sup> and CV curves recorded at scan rates of 5–500 mV/s. Figure 4B compares the dependencies between the anodic peak current ( $I_p$ ) and the square root of scan rate ( $v^{1/2}$ ) on the GCE and the Nafion/GCE. The covering surface with the Nafion film reduced the  $A_s$  from  $0.14 \text{ cm}^2$  to  $0.08 \text{ cm}^2$ . Moreover, an effect of the electrode surface modification with the Nafion layer was investigated using electrochemical impedance spectroscopy (EIS). The impedance spectra (Nyquist plots) were recorded at the bare GCE and the Nafion/GCE in the frequency range from 1 MHz to 0.1 Hz, in a solution of 0.1 M KCl and 5 mM  $\text{K}_3[\text{Fe}(\text{CN})_6]$ . The obtained results (Figure 4C) showed that the charge transfer resistance value of the Nafion/GCE ( $11493 \Omega$ ) is significantly higher than for the bare GCE ( $224.9 \Omega$ ). The observed phenomenon of Kyn signals increase with the Nafion surface modification is associated with the cation-exchanger properties of the Nafion layer that enables preconcentration of the cationic form of Kyn (Figure 3F).

#### Electrochemical behaviour of Kyn at the Nafion/GCE

The cyclic voltammograms (CVs) of Kyn ( $2 \mu\text{M}$ ) at the bare GCE and the Nafion/GCE in 0.1 M  $\text{H}_2\text{SO}_4$  are compared in Figure 5A. As it was demonstrated, no anodic peak was obtained at the bare GCE, whereas a well-defined Kyn signal



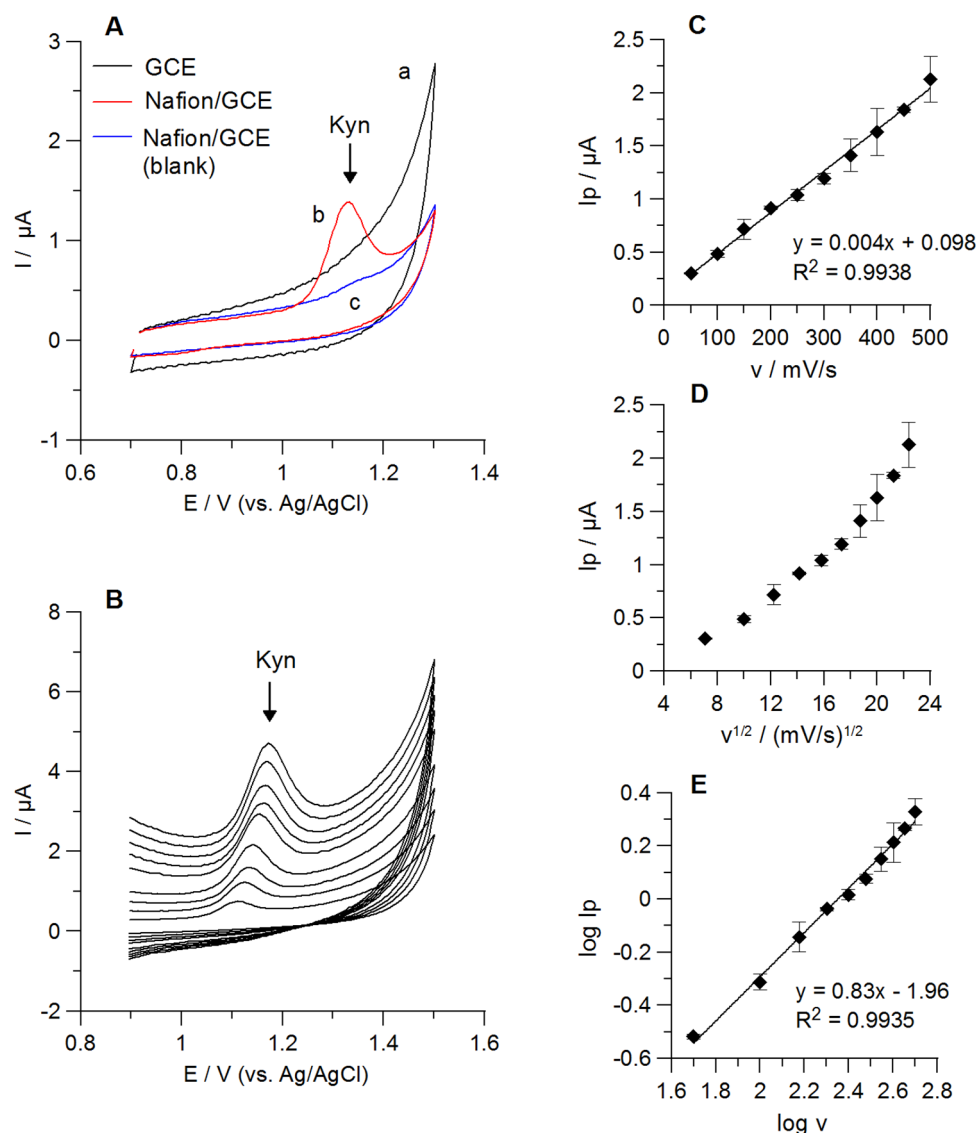


**Figure 5.** Cyclic voltammetric (CV) results of 2  $\mu M$  Kyn in 0.1 M  $H_2SO_4$ . CVs of Kyn at the bare GCE (a) and the Nafion/GCE (b) are shown in panel (A). Curve c: the Nafion/GCE in blank solution; scan rate: 100 mV/s. Panel (B): CVs of Kyn at the Nafion/GCE obtained for different scan rates (50–500 mV/s). Relationships between Kyn anodic peak currents ( $I_p$ ) and the scan rates ( $v$ ) (panel (C)) or square root of the scan rates ( $v^{1/2}$ ) (panel (D)) at the Nafion/GCE are presented. Regression of the logarithm of the Kyn peak currents ( $\log I_p$ ) and the logarithm of the scan rates ( $\log v$ ) is shown in panel (E).

was recorded at the Nafion/GCE. It clearly shows the advantage of GCE surface modification with the Nafion layer in Kyn quantitative analysis.

To further elucidate reactions occurring at the Nafion/GCE in the supporting electrolyte containing 2  $\mu M$  Kyn, the scan rate measurements were carried out from 50 to 500 mV/s in 0.1 M  $H_2SO_4$ . A single Kyn peak in the anodic window and no corresponding peak in the reverse scan were observed suggesting the irreversible oxidation process. This behaviour confirms a shift of Kyn signal toward more positive values with an increase of a scan rate (Figure 5B). The anodic peak currents were linearly proportional to scan rates but not to their square root (Figure 5C and D), suggesting that the electrode process might be controlled by adsorption. Regression of the logarithm of the Kyn peak current ( $\log I_p$ ) and the logarithm of the scan rate ( $\log v$ )

$v$ ) resulted in slopes equal to 0.83 ( $R^2=0.994$ ). This suggests that processes on the Nafion/GCE are controlled by adsorption.<sup>43</sup> Furthermore, the relationship between the Kyn peak positions ( $E_p$ ) and the logarithm of the scan rates ( $\ln v$ ) was linear with a regression equation of  $E_p (V) = 0.03 \ln v (mV/s) + 0.98$  ( $R^2=0.985$ ). This relationship was used for estimation of the number of electrons ( $n$ ) involved in Kyn oxidation process on the Nafion/GCE based on the Laviron's theory.<sup>18</sup> According to this theory, the slope of  $E_p$  versus  $\ln v$  plot is equal to  $RT/\alpha nF$ , where  $R$ —the universal gas constant ( $R=8.314 J mol^{-1} K^{-1}$ ),  $T$ —the absolute temperature ( $T=298 K$ ),  $F$ —Faraday constant ( $F=96 485 C mol^{-1}$ ),  $\alpha$ —transfer coefficient (for irreversible processes  $\alpha=0.5$ ),  $n$ —number of transferred electrons. The obtained  $\alpha n$  value was 0.865, thus the calculated number of transferred electrons was equal to 1.73 ( $\sim 2$ ).

**Table 1.** Comparison of electrochemical sensors for Kyn determination available in literature.

ELECTRODE	TECHNIQUE	LINEAR RANGE [ $\mu\text{M}$ ]	LOD [nM]	APPLICATION	REF.
mAb–MWCNT–AuSPE	CC–PSA	0.001-1.0 1.0-100.0	0.5	Culturing medium from cancer cells	Karami et al. <sup>44</sup>
BiF/BDDE	DPV	0.1-20.0	30.0	Culturing medium from cancer cells	Sadok et al. <sup>18</sup>
Nafion/GCE	DPAAdSV	0.02-10.0 (60s) 0.002-2.0 (600s)	5.1 0.59	Cellular lysate, culturing medium from cancer cells	This work

Abbreviations: DPAAdSV, differential pulse adsorptive stripping voltammetry; BiF/BDDE, boron-doped diamond electrode modified with bismuth nanoparticles; CC-PSA, constant current-potentiometric stripping analysis; DPV, differential pulse voltammetry; mAb–MWCNT–AuSPE, gold screen-printed electrode modified with carboxylated multiwall carbon nanotubes and monoclonal antibody; Nafion/GCE, Nafion film modified glassy carbon electrode.

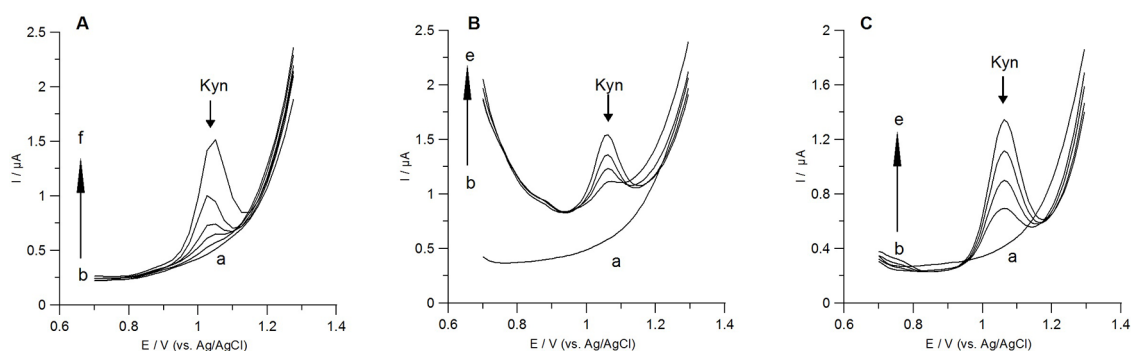


**Figure 6.** (A) DPAdSV curves registered at the Nafion/GCE in 0.1 M  $\text{H}_2\text{SO}_4$  solution containing increasing concentrations of Kyn: (a) 0 nM, (b) 2 nM, (c) 5 nM, (d) 10 nM, (e) 20 nM, (f) 50 nM; accumulation time 600 seconds. (B) and (C) Representative DPAdSV results obtained during Kyn quantification in samples obtained from SK-OV-3 cells (accumulation time 60 seconds). (B) Voltammograms for samples containing cellular lysates for IDO activity estimation (a) background (0.1 M  $\text{H}_2\text{SO}_4$ ), (b) sample in 0.1 M  $\text{H}_2\text{SO}_4$  (60  $\mu\text{L}$ ), (c) as in (b) + 0.08  $\mu\text{M}$  Kyn, (d) as in (b) + 0.12  $\mu\text{M}$  Kyn, (e) as in (b) + 0.24  $\mu\text{M}$  Kyn. (C) DPAdSV curves for samples of culturing medium from cancer cells: (a) background (0.1 M  $\text{H}_2\text{SO}_4$ ), (b) sample in 0.1 M  $\text{H}_2\text{SO}_4$  (15  $\mu\text{L}$ ), (c) as in (b) + 0.2  $\mu\text{M}$  Kyn, (d) as in (b) + 0.4  $\mu\text{M}$  Kyn, (e) as in (b) + 0.6  $\mu\text{M}$  Kyn.

### Calibration graphs, precision, recovery

Linearity of the method was investigated for two accumulation times: 60 and 600 seconds. The obtained calibration graphs were compliant with the equations  $y = 2.90x + 0.18$  ( $R^2 = 0.999$ ) and  $y = 14.84x + 0.22$  ( $R^2 = 0.999$ ) for the accumulation time of 60 and 600 seconds, respectively, where  $y$  corresponds to Kyn peak current ( $\mu\text{A}$ ) and  $x$  is the Kyn concentration ( $\mu\text{M}$ ). The calculated sensitivities were  $36.25 \mu\text{A}\mu\text{M}^{-1}\text{cm}^{-2}$  and  $185.50 \mu\text{A}\mu\text{M}^{-1}\text{cm}^{-2}$  for the accumulation times of 60 and 600 seconds, respectively. Linear ranges are collected in Table 1. The calculated LODs and LOQs were 5.10 and 16.89 nM for the accumulation time of 60 seconds, and 0.59 and 1.96 nM for the accumulation time of 600 seconds, respectively. For the Kyn accumulation time of 600 seconds the Nafion/GCE the similar LOD to that reported for a screen-printed electrode modified by multiwall carbon nanotubes with monoclonal antibody was achieved (Table 1) but without laborious sensor preparation.<sup>44</sup> Furthermore, we achieved better LOD for Kyn compared to that reported by our group at the BiF/BDDE despite a short accumulation time of 60 seconds.<sup>18</sup> An example of voltammograms obtained for low concentrations of Kyn at the Nafion/GCE and the accumulation time 600 seconds are presented in Figure 6A.

Moreover, the herein described electrochemical methodology provided similar or even better LODs for Kyn compared to other sensors and methods using more sophisticated apparatus (Table 2).

Precision was evaluated in the supporting electrolyte containing 0.5  $\mu\text{M}$  Kyn. The established values of intraday and interday precision were 2.82% ( $n = 10$ ) and 4.86% ( $n = 30$ ), respectively. The obtained results did not exceed 5% and confirm good repeatability and reproducibility of the measurements at the Nafion/GCE. The sensor stability was determined for the Nafion/GCE stored on bench-top for the week at ambient conditions. The mean peak current of Kyn ( $n = 8$ ) retains 126.85% of its original value. Regarding the intermediate stability of the sensor, we recommend working with freshly prepared Nafion/GCE. This should not be a problem considering very simple protocol of the electrode surface modification.

Recovery studies were carried out in the presence of sample matrix components. Volumes of culture medium and IDO reaction mixture added to the supporting electrolyte are collected in Table 3 and correspond to these applied in analysis of experimental samples. Recoveries from 91.80% to 112.14% were obtained for both studied matrices.

**Table 2.** Analytical approaches for Kyn determination.

APPROACH	MECHANISM OF DETECTION	LINEAR RANGE [ $\mu$ M]	LOD [nM]	APPLICATION	REF.
LC-UV/FD	UV/Fluorescent detection	0.24-2.88	62.91	Urine	Sousa et al. <sup>45</sup>
LC-Q	Electrospray ionization of the sample	0.01-3.84	3.31	Post-culture medium from cancer cells	Sadok et al. <sup>40</sup>
LC-QQQ	Electrospray ionization of the sample	0.002-7.68	0.68	Cerebrospinal fluid, serum	Eser et al. <sup>46</sup>
GC-QQQ	Chemical ionization of the sample	0.01-1.0	–	Brain	Notarangelo et al. <sup>47</sup>
CE-DAD	Absorbance measurement	1.0-16.0	150.0	Plasma	Zinellu et al. <sup>48</sup>
2D Photonic crystal hydrogel sensor	Diffraction under laser light	0.05-1.0	50.0	Serum	Rizvi et al. <sup>12</sup>
Luminescence chemosensor	Luminescence measurements	1.0-10.0	1.0	–	Tang et al. <sup>49</sup>

Abbreviations: CE-DAD, capillary electrophoresis with a diode array detector; GC-QQQ, gas chromatography coupled to a triple quadrupole mass spectrometer; LC-UV/FD, liquid chromatography coupled to an ultraviolet/visible and a fluorescence detector; LC-Q, liquid chromatography coupled to a single quadrupole mass spectrometer; LC-QQQ, liquid chromatography coupled to a triple quadrupole mass spectrometer.

**Table 3.** Kyn recovery in presence of culturing medium from cancer cells or cellular lysates used for IDO activity (accumulation time: 60 seconds).

AMOUNT ADDED [nM]	AMOUNT FOUND [nM] $\pm$ SD (n=3)	RECOVERY [%]	VOLUME OF THE BIOLOGICAL SAMPLE ADDED ( $\mu$ L) <sup>a</sup>
Sample type: cellular lysate			
20.00	22.56 $\pm$ 1.31	112.78	40
40.00	44.86 $\pm$ 3.29	112.14	40
Sample type: culturing medium			
80.00	73.44 $\pm$ 5.71	91.80	10
600.00	554.41 $\pm$ 82.10	92.40	50

Abbreviation: SD, standard deviation.

<sup>a</sup>Volume of the supporting electrolyte was 5 mL.

### Selectivity

An effect of various interfering compounds on 0.5  $\mu$ M Kyn voltammetric response at the Nafion/GCE was investigated in the range of 0.05 – 1000  $\mu$ M. The concentration of the interfering compound that causes no more than  $\pm$  10% change in Kyn peak current was considered as tolerable. The obtained results are collected in Table 4.

The major pathway of dietary Trp catabolism is the kynurenine pathway, which produces Kyn and other biologically active metabolites so-called kynurenines accumulating in tissues. Therefore, the interference of different kynurenines on the Kyn voltammetric response was also investigated. Under applied conditions, quinolinic acid (QA) and picolinic acid (PIC) generated no voltammetric signals at the Nafion/GCE and had no effect on Kyn signal over the studied concentration range. Signals of kynurenic acid (Kyna), 3-hydroxyanthranilic acid (3HAA) did not appear at the Nafion/GCE in the potential window

from +0.7 to +1.3 V, whereas xanthurenic acid (XA), 3-hydroxykynurenine (3HKyn), anthranilic acid (AA) resulted in voltammetric peaks at about +0.85, +0.93, +1.0 V, respectively. These kynurenines have shown a tendency to decrease Kyn signal (with AA being an exception) with estimated tolerance limits collected in Table 4. It is worth noting that in different biological samples Kyn is usually present at substantially higher concentrations compared to other downstream metabolites. For example, in serum from healthy donors, 25 to 100-fold excess of Kyn compared to Kyna, 3HAA, 3HKyn, XA, AA has been noted.<sup>50,51</sup> Furthermore, other kynurenines are not detected or hardly detected in the post-culture medium collected from different types of cancer cells.<sup>40,52-54</sup> In some conditions, that is, IFN- $\gamma$  stimulation, Trp metabolism is accelerated generating both Kyn and downstream kynurenines secretion.<sup>52,54</sup>

In addition to oxidation occurring within the kynurenine pathway, in a cell, Trp might undergo hydroxylation, decarboxylation, or transamination to yield other biologically important

**Table 4.** Tolerable excess of different organic compounds on Kyn (0.5  $\mu$ M) voltammetric signal.

INTERFERING COMPOUNDS	TOLERABLE EXCESS
Kynurenine pathway metabolites	
QA, PIC	2000-fold
Kyna	1000-fold
3HAA	100-fold
XA	40-fold
3HKyn	10-fold
AA	Equal concentration
Other tryptophan metabolites	
ME	100-fold
IA, 5HIAA	10-fold
IS	4-fold
5-HT	2-fold
Amino acids	
Ala, Asn, Asp, Gly, Glu, Leu, Phe, Pro, Ser, Thr, Val	2000-fold
Lys	1000-fold
Arg, Cys, His	200-fold
Trp, Met	40-fold
Tyr	4-fold
Others	
Glucose, TA, LA, NAm, NA	2000-fold
OA, CA	1000-fold
UA	200-fold
Vit C, DOP	10-fold

compounds.<sup>2</sup> Therefore, the effect of other Trp metabolites on Kyn peak current was studied, and the estimated thresholds were summarized in Table 4. Indoxyl acetate (IA) and indoxyl sulfate (IS) enhanced Kyn signal, whereas melatonin (ME), 5-hydroxyindoleacetic acid (5HIAA), 5-hydroxytryptamine (serotonin, 5-HT) decreased the target analyte peak current. However, Kyn signal was still measurable up to 10-, 100-, and 400-fold excess of 5-HT, 5HIAA, ME, respectively. The amount of these metabolites in the different biological samples might vary depending on cellular conditions and pathological state, that is, in human serum (healthy donors) IS, IA 5-HT, ME are present at similar or below Kyn level.<sup>51,55,56</sup> In human plasma, 5HT, 5HIAA, ME amounts are much lower than Kyn.<sup>56,57</sup> Therefore, the method accuracy in the biological matrix of interest needs to be verified using a comparative method.

The sensor was developed for Kyn determination in culturing medium from cancer cells that consists of essential amino

**Table 5.** Comparison of DPAdSV and HPLC-DAD methods for determination of IDO activity (Kyn generated by IDO present in cellular extracts) or Kyn secreted into culturing medium collected from a culture of SK-OV-3 cells.

SAMPLE TYPE: CELLULAR LYSATE			
IDO ACTIVITY $\pm$ SD [NMOL KYN/MIN/MG PROTEIN]			
SAMPLE	DPADSV	HPLC-DAD	P VALUE
1	1.19 $\pm$ 0.16	1.35 $\pm$ 0.15	0.349
2	4.48 $\pm$ 0.39	4.93 $\pm$ 0.18	0.233
3	0.63 $\pm$ 0.03	0.69 $\pm$ 0.03	0.086
4	0.73 $\pm$ 0.05	0.78 $\pm$ 0.07	0.411
SAMPLE TYPE: CULTURING MEDIUM FROM CANCER CELLS			
KYN CONCENTRATION $\pm$ SD [ $\mu$ M]			
5	56.00 $\pm$ 8.29	60.65 $\pm$ 0.35	0.507
6	126.22 $\pm$ 3.58	130.783 $\pm$ 1.17	0.194
7	84.11 $\pm$ 1.76	84.04 $\pm$ 1.16	0.859
8	51.96 $\pm$ 7.05	55.38 $\pm$ 0.60	0.563
9	53.73 $\pm$ 2.11	53.54 $\pm$ 0.51	0.913
10	124.95 $\pm$ 4.72	122.38 $\pm$ 2.66	0.546

Abbreviation: SD, standard deviation from n=3 (DPAdSV) or n=2 (HPLC-DAD) measurements.

acids, sugars, vitamins, and other protein factors necessary for the growth of cells. The sensor shows good selectivity towards majority of the tested amino acids (Table 4) in the culturing medium. The lowest tolerance limits were estimated for tryptophan (Trp), methionine (Met), and tyrosine (Tyr), whereas Trp, Met decreased and Tyr increased Kyn signal. It should be noted that 2000-fold excess of Met suppressed Kyn peak current by 50%. Glucose did not interfere with Kyn measurement over the studied concentration range, whereas more than 10-fold excess of ascorbic acid (Vit C) significantly increased Kyn peak current (>10%). Dopamine (DOP) decreased the target analyte peak current, but Kyn signal was still measurable up to 1000-fold excess of this compound. Nicotinamide (NAm) and nicotinic acid (NA) had no effect on Kyn signal over the studied concentration range. Furthermore, the sensor has shown satisfactory selectivity towards oxalic acid (OA), tartaric acid (TA), citric acid (CA), and lactic acid (LA). Uric acid (UA) significantly suppressed Kyn signal with an excess greater than 200-fold, wherein 2000-fold excess of UA reduced Kyn peak current by about 50%.

### Method Application

The herein presented voltammetric method was applied for Kyn quantification in material derived from SK-OV-3 human ovarian carcinoma cells. First, we attempted to measure IDO

enzyme activity in cancer cell extracts. It was set up to determine the amount of L-Kyn (nmol) produced from L-Trp (substrate) within 1 hour.<sup>39</sup> The generated Kyn was quantified using DPAdSV and HPLC-DAD methods in cellular lysate extract as described in Material and Methods. The obtained results were further normalized by protein content (determined in mg by Bradford's method) to consider cell number and reaction time (60 minutes). IDO activity in random samples of SK-OV-3 cells determined by DPAdSV ranged from 0.63 to 4.48 nmol Kyn/min/mg protein (Table 5). The examples of voltammograms recorded for Kyn determination are presented in Figure 6B. The results are in good accordance with measurements obtained by HPLC-DAD used as a reference method. There were no statistically important differences between results obtained by both methods calculated with *t*-test (all *P* values >.05).

We have also employed the Nafion/GCE to measure Kyn secreted into the culture medium by SK-OV-3 cells. In six analysed samples, Kyn concentration ranged from 51.96 to 126.22 μmol/L (Table 5). Similar results have been noted in our previous studies using the BiF/BDDE as a working electrode (31–58 μmol/L).<sup>18</sup> As demonstrated in Figure 6C, none of culture medium components nor other metabolites produced by the cancer cells affected the voltammetric signal from Kyn. Furthermore, the accuracy of the obtained results was confirmed by HPLC-DAD method. The *t*-test did not show a statistically important difference between Kyn levels in the culturing medium from cancer cells when measured by DPAdSV and HPLC-DAD (all *P* values >.05).

## Conclusion

Herein, we reported for the first time the advantages of the Nafion-based voltammetric sensor for kynurenine determination in biological samples. The sensor applicability was tested in two types of samples delivered from SK-OV-3 human ovarian cancer cells. Despite the complex composition of a culturing medium collected from cells and the cellular lysates, the voltammetric determination of Kyn at the Nafion/GCE was easy to perform and provided accurate data (confirmed by HPLC-DAD). A basal level of IDO activity in SK-OV-3 cancer cells ranged from 0.63 to 4.48 nmol L-Kyn/min/mg protein, while the amount of Kyn secreted by the cells into the culture medium was in the range of 51.96–126.22 μM. It is worth mentioning that in this work Kyn determination in the real samples was performed with the accumulation time of 60 seconds. However, to obtain higher sensitivity, the accumulation time can be prolonged up to 600 seconds. Importantly, the Nafion/GCE allows for the determination of lower concentrations of Kyn comparing to previously proposed by our group sensor - the BiF/BDDE. It brings a benefit to significantly reduce a volume of the tested sample that is needed for voltammetric measurements of Kyn (from 200–500 μL to 5–50 μL of culturing medium from cancer cells for the BiF/BDDE and the Nafion/GCE, respectively). Comparing to

HPLC-DAD, Kyn determination by DPAdSV at the Nafion/GCE can be conducted with good accuracy and with no need for time-consuming separation of the sample components onto the analytical column. Unlike HPLC-DAD, the DPAdSV measurements were carried out only in aqueous solutions, and the usage of organic solvents is minimal (dissolving crystalline analyte standards or diluting Nafion solution). Furthermore, for the analysis of cell culturing medium, the sample preparation step can be omitted. These findings demonstrate that DPAdSV measurements at the Nafion/GCE hold promise as a new tool for a rapid determination of low amounts of Kyn in samples delivered from *in vitro* cultured cells.

## Acknowledgements

The authors gratefully acknowledge access to the tissue culture equipment within the Laboratory of Oxidative Stress at the Centre for Interdisciplinary Research, John Paul II Catholic University of Lublin, Poland.

## Author Contributions

Conceptualization: I.S.; Investigation: I.S., R.M., J.K.; Methodology: I.S., K.T.-R., R.M., M.S.; Supervision: K.T.-R. and M.S.; Validation: I.S.; Visualization: I.S.; Writing – original draft: I.S.; Writing - review & editing: I.S., K.T.-R., R.M., M.S.

## ORCID iDs

Ilona Sadok  <https://orcid.org/0000-0003-1154-7581>

Magdalena Staniszewska  <https://orcid.org/0000-0003-1119-2397>

## REFERENCES

- Munn DH, Mellor AL. IDO in the tumor microenvironment: inflammation, counter-regulation, and tolerance. *Trends Immunol.* 2016;37:193–207.
- Badawy AA-B. Tryptophan metabolism, disposition and utilization in pregnancy. *Biosci Rep.* 2015;35:e00261.
- Eastman CL, Guilarte TR. Cytotoxicity of 3-hydroxykynurenine in a neuronal hybrid cell line. *Brain Res.* 1989;495:225–231.
- Guillemin GJ. Quinolinic acid, the inescapable neurotoxin. *FEBS J.* 2012;279:1325–1365.
- Frumento G, Rotondo R, Tonetti M, Damonte G, Benatti U, Ferrara GB. Tryptophan-derived catabolites are responsible for inhibition of T and natural killer cell proliferation induced by indoleamine 2,3-dioxygenase. *J Exp Med.* 2002;196:459–468.
- Opitz CA, Litzzenburger UM, Sahn F, et al. An endogenous tumour-promoting ligand of the human aryl hydrocarbon receptor. *Nature.* 2011;478:197–203.
- Huengsborg M, Winer JB, Compels M, Round R, Ross J, Shahmanesh M. Serum kynurenine-to-tryptophan ratio increases with progressive disease in HIV-infected patients. *Clin Chem.* 1998;44:858–862.
- Suzuki Y, Suda T, Furuhashi K, et al. Increased serum kynurenine/tryptophan ratio correlates with disease progression in lung cancer. *Lung Cancer.* 2010;67:361–365.
- Zinellu A, Fois AG, Zinellu E, et al. Increased kynurenine plasma concentrations and kynurenine-tryptophan ratio in mild-to-moderate chronic obstructive pulmonary disease patients. *Biomark Med.* 2018;12:229–237.
- Evangelisti M, De Rossi P, Rabasco J, et al. Changes in serum levels of kynurenine metabolites in paediatric patients affected by ADHD. *Eur Child Adolesc Psychiatry.* 2017;26:1433–1441.
- Sadok I, Gamian A, Staniszewska MM. Chromatographic analysis of tryptophan metabolites. *J Sep Sci.* 2017;40:3020–3045.
- Rizvi AS, Murtaza G, Yan D, et al. Development of molecularly imprinted 2D photonic crystal hydrogel sensor for detection of L-Kynurenine in human serum. *Talanta.* 2020;208:120403–120412.

13. Klockow JL, Glass TE. Development of a fluorescent chemosensor for the detection of kynurenine. *Org Lett.* 2013;15:235-237.
14. Li G, Xia Y, Tian Y, et al. Review—recent developments on graphene-based electrochemical sensors toward nitrite. *J Electrochem Soc.* 2019;166:B881-B895.
15. Li Q, Xia Y, Wan X, et al. Morphology-dependent MnO<sub>2</sub>/nitrogen-doped graphene nanocomposites for simultaneous detection of trace dopamine and uric acid. *Mater Sci Eng C.* 2020;109:110615-110626.
16. Li G, Zhong P, Ye Y, et al. A highly sensitive and stable dopamine sensor using shuttle-like  $\alpha$ -Fe<sub>2</sub>O<sub>3</sub> nanoparticles/electro-reduced graphene oxide composites. *J Electrochem Soc.* 2019;166:B1552-B1561.
17. Liu H, Xiong R, Zhong P, et al. Nanohybrids of shuttle-like  $\alpha$ -Fe<sub>2</sub>O<sub>3</sub> nanoparticles and nitrogen-doped graphene for simultaneous voltammetric detection of dopamine and uric acid. *New J Chem.* 2020;44:20797-20805.
18. Sadok I, Tyszczyk-Rotko K, Mroccka R, Staniszevska M. Simultaneous voltammetric analysis of tryptophan and kynurenine in culture medium from human cancer cells. *Talanta.* 2020;209:120574-120585.
19. Yue W, Bange A, Riehl BL, et al. Manganese detection with a metal catalyst free carbon nanotube electrode: anodic versus cathodic stripping voltammetry. *Electroanalysis.* 2012;24:1909-1914.
20. Nagles E, Arancibia V, Rojas C, Segura R. Nafion-mercury coated film electrode for the adsorptive stripping voltammetric determination of lead and cadmium in the presence of pyrogallol red. *Talanta.* 2012;99:119-124.
21. Torma F, Grün A, Bitter I, Tóth K. Calixarene/Nafion-modified bismuth-film electrodes for adsorptive stripping voltammetric determination of lead. *Electroanalysis.* 2009;21:1961-1969.
22. Meepon N, Siriket S, Dejmanee S. Adsorptive stripping voltammetry for determination of cadmium in the presence of cupferron on a Nafion-coated bismuth film electrode. *Int J Electrochem Sci.* 2012;7:10582-10591.
23. Katowah DF, Hussein MA, Alam MM, et al. Designed network of ternary core-shell PPCOT/NiFe<sub>2</sub>O<sub>4</sub>/C-SWCNTs nanocomposites. A selective Fe<sup>3+</sup> ionic sensor. *J Alloys Compd.* 2020;834:155020-155036.
24. Aqlan FM, Alam MM, Al-Bogami AS, et al. Efficient electro-chemical sensor for sensitive Cd<sup>2+</sup> detection based on novel in-situ synthesized hydrazoneyl bromide (HB). *J Mol Struct.* 2021;1231:129690-129699.
25. Rahman MM, Ahmed J, Asiri AM, Alamry KA. Fabrication of a hydrazine chemical sensor based on facile synthesis of doped NZO nanostructure materials. *New J Chem.* 2020;44:13018-13029.
26. Subhan MA, Chandra Saha P, Ahmed J, Asiri AM, Al-Mamun M, Rahman MM. Development of an ultra-sensitive para-nitrophenol sensor using tri-metallic oxide MoO<sub>2</sub>·Fe<sub>2</sub>O<sub>4</sub>·CuO nanocomposites. *Mater Adv.* 2020;1:2831-2839.
27. Abu-Zied BM, Alam MM, Asiri AM, Ahmed J, Rahman MM. Efficient hydroquinone sensor development based on Co<sub>3</sub>O<sub>4</sub> nanoparticle. *Microchem J.* 2020;157:104972-104981.
28. Rahman MM, Ahmed J, Asiri AM. Selective bilirubin sensor fabrication based on doped IAO nanorods for environmental remediation. *New J Chem.* 2019;43:19298-19307.
29. Rahman MM, Ahmed J, Asiri AM. Thiourea sensor development based on hydrothermally prepared CMO nanoparticles for environmental safety. *Biosens Bioelectron.* 2018;99:586-592.
30. Rahman MM, Ahmed J. Cd-doped Sb<sub>2</sub>O<sub>3</sub> nanostructures modified glassy carbon electrode for efficient detection of melamine by electrochemical approach. *Biosens Bioelectron.* 2018;102:631-636.
31. Ahmed J, Rahman MM, Siddiquey IA, Asiri AM, Hasnat MA. Efficient Bisphenol-A detection based on the ternary metal oxide (TMO) composite by electrochemical approaches. *Electrochim Acta.* 2017;246:597-605.
32. Rahman MM, Ahmed J, Asiri AM. Development of Creatine sensor based on antimony-doped tin oxide (ATO) nanoparticles. *Sens Actuators B Chem.* 2017;242:167-175.
33. Ahmed J, Rahman MM, Siddiquey IA, Asiri AM, Hasnat MA. Efficient hydroquinone sensor based on zinc, strontium and nickel based ternary metal oxide (TMO) composites by differential pulse voltammetry. *Sens Actuators B Chem.* 2018;256:383-392.
34. Tyszczyk-Rotko K, Bęczkowska I. Nafion covered lead film electrode for the voltammetric determination of caffeine in beverage samples and pharmaceutical formulations. *Food Chem.* 2015;172:24-29.
35. Yi H, Wu K, Hu S, Cui D. Adsorption stripping voltammetry of phenol at Nafion-modified glassy carbon electrode in the presence of surfactants. *Talanta.* 2001;55:1205-1210.
36. Desai PB, Srivastava AK. Adsorptive stripping differential pulse voltammetric determination of metoprolol at Nafion-CNT-nano-composite film sensor. *Sens Actuators B Chem.* 2013;176:632-638.
37. Sadok I, Rachwał K, Staniszevska M. Simultaneous quantification of selected kynurenines analyzed by liquid chromatography-mass spectrometry in medium collected from cancer cell cultures. *J Vis Exp.* 2020;159:e61031-e61040.
38. Mailankot M, Staniszevska MM, Butler H, et al. Indoleamine 2,3-dioxygenase overexpression causes kynurenine-modification of proteins, fiber cell apoptosis and cataract formation in the mouse lens. *Lab Invest.* 2009;89:498-512.
39. Sadok I, Rachwał K, Jonik I, Staniszevska M. Reliable chromatographic assay for measuring of indoleamine 2,3-dioxygenase 1 (IDO1) activity in human cancer cells. *J Enzyme Inhib Med Chem.* 2021;36:581-592.
40. Sadok I, Rachwał K, Staniszevska M. Application of the optimized and validated LC-MS method for simultaneous quantification of tryptophan metabolites in culture medium from cancer cells. *J Pharm Biomed Anal.* 2019;176:112805-112815.
41. Tömösi F, Kecskeméti G, Cseh EK, et al. A validated UHPLC-MS method for tryptophan metabolites: application in the diagnosis of multiple sclerosis. *J Pharm Biomed Anal.* 2020;185:113246-113258.
42. Sipa K, Brycht M, Leniart A, et al.  $\beta$ -Cyclodextrins incorporated multi-walled carbon nanotubes modified electrode for the voltammetric determination of the pesticide dichlorophen. *Talanta.* 2018;176:625-634.
43. Shayani-jam H. Electrochemical study of adsorption and electrooxidation of 4,4'-biphenol on the glassy carbon electrode: determination of the orientation of adsorbed molecules. *Monatsh Chem.* 2019;150:183-192.
44. Karami P, Majidi MR, Johari-Ahar M, Barar J, Omid Y. Development of screen-printed tryptophan-kynurenine immunosensor for in vitro assay of kynurenine-mediated immunosuppression effect of cancer cells on activated T-cells. *Biosens Bioelectron.* 2017;92:287-293.
45. Sousa A, Ribeiro C, Gonçalves VMF, et al. Development and validation of a liquid chromatography method using UV/fluorescence detection for the quantitative determination of metabolites of the kynurenine pathway in human urine: application to patients with heart failure. *J Pharm Biomed Anal.* 2021;198:113997-114006.
46. Eser B, Özkan Y, Sepici Dinçel A. Determination of tryptophan and kynurenine by LC-MS/MS by using amlodipine as an internal standard. *J Am Soc Mass Spectrom.* 2020;31:379-385.
47. Notarangelo FM, Wu HQ, Macherone A, Graham DR, Schwarcz R. Gas chromatography/tandem mass spectrometry detection of extracellular kynurenine and related metabolites in normal and lesioned rat brain. *Anal Biochem.* 2012;421:573-581.
48. Zinellu A, Sotgia S, Deiana L, Talanas G, Terrosu PF, Carru C. Simultaneous analysis of kynurenine and tryptophan in human plasma by capillary electrophoresis with UV detection. *J Sep Sci.* 2012;35:1146-1151.
49. Tang T, Liu M, Chen Z, et al. Highly sensitive luminescent lanthanide metal-organic framework sensor for L-kynurenine. *J Rare Earths.* Published online February 20, 2021. doi:10.1016/j.jre.2021.02.008
50. Sakurai M, Yamamoto Y, Kanayama N, et al. Serum Metabolic Profiles of the Tryptophan-Kynurenine Pathway in the high risk subjects of major depressive disorder. *Sci Rep.* 2020;10:1961.
51. Zhang A, Rijal K, Ng SK, Ravid K, Chitalia V. A mass spectrometric method for quantification of tryptophan-derived uremic solutes in human serum. *J Biol Methods.* 2017;4:e75.
52. Yamada K, Miyazaki T, Shibata T, Hara N, Tsuchiya M. Simultaneous measurement of tryptophan and related compounds by liquid chromatography/electrospray ionization tandem mass spectrometry. *J Chromatogr B Analyt Technol Biomed Life Sci.* 2008;867:57-61.
53. Zhu W, Stevens A, Dettmer K, et al. Quantitative profiling of tryptophan metabolites in serum, urine, and cell culture supernatants by liquid chromatography-tandem mass spectrometry. *Anal Bioanal Chem.* 2011;401:3249-3261.
54. Guillemain GJ, Cullen KM, Lim CK, et al. Characterization of the kynurenine pathway in human neurons. *J Neurosci.* 2007;27:12884-12892.
55. Moriarty M, Lee A, O'Connell B, Lehane M, Keeley H, Furey A. The application and validation of HybridSPE-Precipitation cartridge technology for the rapid clean-up of serum matrices (from phospholipids) for the clinical analysis of serotonin, dopamine and melatonin. *Chromatographia.* 2012;75:1257-1269.
56. Hsing AW, Meyer TE, Niwa S, Quraishi SM, Chu LW. Measuring serum melatonin in epidemiologic studies. *Cancer Epidemiol Biomarkers Prev.* 2010;19:932-937.
57. Chen Y, Chen H, Shi G, et al. Ultra-performance liquid chromatography-tandem mass spectrometry quantitative profiling of tryptophan metabolites in human plasma and its application to clinical study. *J Chromatogr B Analyt Technol Biomed Life Sci.* 2019;1128:121745-121757.